

NUMERICAL OPERATIONAL CALCULUS FOR
MATRICES WITH APPLICATIONS TO
MECHANICAL AND MATHEMATICAL PROBLEMS

L. KOHAUPT

ABSTRACT. The calculation of the matrix exponential e^A is important in many problems of mechanics and applied mathematics. In this paper its calculation is based on the Dunford-Taylor integral representation. As a contour line, a polygonal is chosen where the eigenvalues of A lie in its interior, the contour integral is evaluated numerically by a summed Gaussian quadrature formula, and estimates of the discretization error for a mechanical problem are given which are optimal in a certain sense, and which prove the convergence of the described method. It is shown theoretically that the method – called Numerical Operational Calculus – is superior to the methods known so far for sparse matrices of large order, a situation which often occurs in applications. The theoretical considerations are confirmed by numerical tests for the free-vibration problem of a multi-mass vibration chain. We stress that the damping matrix need not be proportional to the mass and/or stiffness matrix. Also, the method is applied to a series of problems from mathematics showing its wide range of applicability.

0. Introduction. The calculation of matrix functions by contour integrals has been widely used in recent years for problems from physics (cf., e.g., [1], [5] and [13]).

In this paper, we want to carry over this method to the computation of the fundamental matrix, which has not yet been done, as far as we know. As opposed to [1], [5] and [13], we give estimates for the discretization error.

The paper contains two chapters, namely Chapter I: Theory and Chapter II: Applications. Chapter I consists of Sections 1 and 2, and Chapter II of Sections 3 and 4.

In Section 1, we start with Cauchy's integral theorem and the numerical evaluation of the integral over an interval, followed by a summed quadrature formula and the evaluation of the contour integral over a closed polygonal. These results serve as a preparation to the next section.

In Section 2, a matrix function is defined as the Dunford-Taylor integral. The associated numerical evaluation is done by simply rewriting the results of Section 1. The numerical process is called here *Numerical Operational Calculus*.

Section 3 contains the main example for the theory developed in Sections 1 and 2. From the many tasks involving the computation of the matrix exponential we choose the free-vibration problem of a multi-mass vibration chain. First, the model is set up. Then, the method – the Numerical Operational Calculus – is described, the discretization error is estimated and the theoretical advantages over the other methods for sparse matrices with large dimensions are exhibited. Finally, the theoretical considerations are confirmed by test computations.

In Section 4 we demonstrate the applicability of the method to some mathematical problems such as an example of e^A of Stickel, the spectral decomposition of a matrix with well-separated eigenvalues and the square root of a positive definite matrix. In these examples, we do not claim that the described method is superior to other ones, but we want to illustrate that it can be used in a whole series of mathematical problems in a straightforward manner.

We remark that the submatrices M , B and K of the system matrix A are assumed to be sparse only in the numerical computations.

1. Gaussian quadrature formula for analytic functions.

In Kato [8, pp. 34–47], statements on operator functions in finite dimensional spaces are obtained by just rewriting corresponding results from the theory of analytic functions (cf. Knopp [9]). Since this makes the presentation quite clear, we follow the same line here. So, in this section, quadrature formulae for the evaluation of contour integrals with complex integrands are derived, which we rewrite for matrix functions in the next section.

1.1 Simple quadrature formula on interval. The starting point of our investigation is

Cauchy's integral formula. If $f(z)$ is analytic inside and on a simple

curve Γ , then

$$(1) \quad f(z) = \frac{1}{2\pi i} \int_{\Gamma} \frac{f(\lambda)}{\lambda - z} d\lambda$$

where Γ is traversed in the positive (counterclockwise) sense (cf. Knopp [9, p. 64]).

In Subsection 1.2, for Γ we choose a polygonal. As a preparatory step, in this subsection we select an interval $[a, b]$ in the complex plane as integration path.

In order to compute the integral over $[a, b]$, we first introduce the parameter s so that

$$(2) \quad \lambda(s) = a + s(b - a), \quad 0 \leq s \leq 1.$$

Then

$$(3) \quad I(f(z))_{[a,b]} := \frac{1}{2\pi i} \int_a^b \frac{f(\lambda)}{\lambda - z} d\lambda = \int_0^1 g(s) ds$$

with

$$(4) \quad g(s) = \frac{b - a}{2\pi i} \frac{f(\lambda(s))}{\lambda(s) - z}, \quad 0 \leq s \leq 1.$$

In order to evaluate the integral in (3) numerically, we apply a quadrature formula. The three-knot Gaussian quadrature formula, e.g., follows from Stummel and Hainer [16, pp. 84–88].

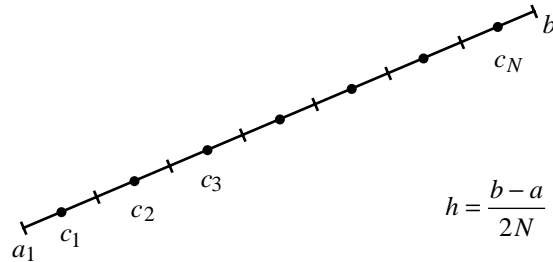
We obtain

*Gauss*₃:

$$Q(g) = \frac{1}{18} \left[5g\left(s_c - s_h \frac{\sqrt{15}}{5}\right) + 8g(s_c) + 5g\left(s_c + s_h \frac{\sqrt{15}}{5}\right) \right]$$

with $s_c = (s_a + s_b)/2 = 1/2$, $s_h = (s_b - s_a)/2 = 1/2$ or

$$\begin{aligned} & Q(f(z))_{[a,b]} \\ &= \frac{b - a}{2\pi i} \frac{1}{18} \left[5 \frac{f(c - h(\sqrt{15}/5))}{(c - h(\sqrt{15}/5)) - z} + 8 \frac{f(c)}{c - z} + 5 \frac{f(c + h(\sqrt{15}/5))}{(c + h(\sqrt{15}/5)) - z} \right] \end{aligned}$$

FIGURE 1. N subintervals.

with $h = (b - a)/2$, $c = (a + b)/2$, and

$$|E(g)| \leq \frac{1}{2016000} \max_{s_a \leq s \leq s_b} |g^{(6)}(s)|.$$

For the error estimates, one needs the sixth derivative of g which now follows:

$$\begin{aligned} & \frac{d^6 g(s)}{ds^6} \\ &= \frac{(b-a)^7}{2\pi i} \left[\frac{d^6 f(\lambda(s))}{d\lambda^6} \frac{1}{\lambda(s)-z} - 6 \frac{d^5 f(\lambda(s))}{d\lambda^5} \frac{1}{(\lambda(s)-z)^2} \right. \\ & \quad + 30 \frac{d^4 f(\lambda(s))}{d\lambda^4} \frac{1}{(\lambda(s)-z)^3} - 120 \frac{d^3 f(\lambda(s))}{d\lambda^3} \frac{1}{(\lambda(s)-z)^4} \\ & \quad + 360 \frac{d^2 f(\lambda(s))}{d\lambda^2} \frac{1}{(\lambda(s)-z)^5} - 720 \frac{d f(\lambda(s))}{d\lambda} \frac{1}{(\lambda(s)-z)^6} \\ & \quad \left. + 720 f(\lambda(s)) \frac{1}{(\lambda(s)-z)^7} \right]. \end{aligned}$$

1.2 Summed quadrature formula on interval. In order to increase the accuracy, we subdivide the interval $[a, b]$ into N parts of equal length (cf. Figure 1), thus obtaining a summed Gaussian quadrature formula on the interval $[a, b]$.

Let

$$(5) \quad c_j = a + (2j - 1)h, \quad j = 1, 2, \dots, N; \quad h = \frac{b-a}{2N}.$$

Then,

$$\begin{aligned}
 Q_{G_3}(g) &= Q_{G_3}(f(z))_{[a,b]} \\
 (6) \quad &= \frac{(b-a)/N}{2\pi i} \frac{1}{18} \sum_{j=1}^N \left[5 \frac{f(c_j - h(\sqrt{15}/5))}{(c_j - (\sqrt{15}/5)) - z} + 8 \frac{f(c_j)}{c_j - z} \right. \\
 &\quad \left. + 5 \frac{f(c_j + h(\sqrt{15}/5))}{(c_j + h(\sqrt{15}/5)) - z} \right]
 \end{aligned}$$

or

$$\begin{aligned}
 Q_{G_3}(g) &= Q_{G_3}(f(z))_{[a,b]} \\
 (7) \quad &= \frac{h}{2\pi i} \frac{1}{9} \sum_{j=1}^N \left[5 \frac{f(c_j - h(\sqrt{15}/5))}{(c_j - h(\sqrt{15}/5)) - z} + 8 \frac{f(c_j)}{c_j - z} \right. \\
 &\quad \left. + 5 \frac{f(c_j + h(\sqrt{15}/5))}{(c_j + h(\sqrt{15}/5)) - z} \right]
 \end{aligned}$$

and

$$(8) \quad |E_{G_3}(f(z))_{[a,b]}| = |E_{G_3}(g)| \leq \sum_{k=1}^N \frac{1}{2016000} \max_{(k-1)/N \leq s \leq (k/N)} \left| \frac{d^6 g(s)}{ds^6} \right|.$$

For $(k-1)/N \leq s \leq (k/N)$, one has

$$\begin{aligned}
 (9) \quad &\frac{d^6 g(s)}{ds^6} \\
 &= \frac{((b-a)/N)^7}{2\pi i} \left[\frac{d^6 f(\lambda(s))}{d\lambda^6} \frac{1}{\lambda(s) - z} - 6 \frac{d^5 f(\lambda(s))}{d\lambda^5} \frac{1}{(\lambda(s) - z)^2} \right. \\
 &\quad + 30 \frac{d^4 f(\lambda(s))}{d\lambda^4} \frac{1}{(\lambda(s) - z)^3} - 120 \frac{d^3 f(\lambda(s))}{d\lambda^3} \frac{1}{(\lambda(s) - z)^4} \\
 &\quad + 360 \frac{d^2 f(\lambda(s))}{d\lambda^2} \frac{1}{(\lambda(s) - z)^5} - 720 \frac{d f(\lambda(s))}{d\lambda} \frac{1}{(\lambda(s) - z)^6} \\
 &\quad \left. + 720 f(\lambda(s)) \frac{1}{(\lambda(s) - z)^7} \right].
 \end{aligned}$$

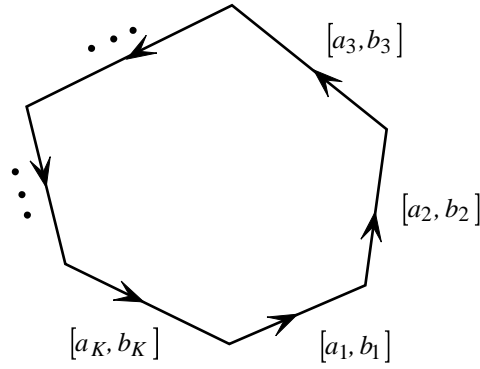


FIGURE 2. Closed polygonal.

Hence,

$$|E_{G_3}(f(z))_{[a,b]}| = |E_{G_3}(g)| \leq \frac{|b-a|^7}{2\pi N^6} \frac{1}{2016000}.$$

$$(10) \quad \max_{s_a \leq s \leq s_b} \left\{ \left| \frac{d^6 f(\lambda(s))}{d\lambda^6} \right| |(\lambda(s)-z)^{-1}| + 6 \left| \frac{d^5 f(\lambda(s))}{d\lambda^5} \right| |(\lambda(s)-z)^{-2}| \right. \\ + 30 \left| \frac{d^4 f(\lambda(s))}{d\lambda^4} \right| |(\lambda(s)-z)^{-3}| + 120 \left| \frac{d^3 f(\lambda(s))}{d\lambda^3} \right| |(\lambda(s)-z)^{-4}| \\ + 360 \left| \frac{d^2 f(\lambda(s))}{d\lambda^2} \right| |(\lambda(s)-z)^{-5}| + 720 \left| \frac{d f(\lambda(s))}{d\lambda} \right| |(\lambda(s)-z)^{-6}| \\ \left. + 720 |f(\lambda(s))| |(\lambda(s)-z)^{-7}| \right\}.$$

1.3 Summed quadrature formula on closed polygonal. If the closed polygonal consists of \$K\$ intervals \$[a_k, b_k]\$, \$k = 1, \dots, K\$ as in Figure 2, one has

$$(11) \quad Q(f(z)) = \sum_{k=1}^K Q(f(z))_{[a_k, b_k]}$$

and

$$(12) \quad |E(f(z))| \leq \sum_{k=1}^K |E(f(z))_{[a_k, b_k]}|.$$

2. Gaussian quadrature formula for matrix functions. In this section we rewrite the results of Sections 1, which are needed here for matrix functions. The quadrature formula and error estimate thus obtained form the basis for the evaluation of the contour integrals, that is, of the numerical operational calculus used in the applications to follow.

2.1 Simple quadrature formula on interval. Let A be an $m \times m$ matrix with elements from \mathbf{C} . Suppose that $f(z)$ is analytic in a domain Δ of the complex plane, and let $\Gamma \subset \Delta$ be a simple closed smooth curve with positive direction enclosing all eigenvalues of A in its interior. Then $f(A)$ is defined by the Dunford-Taylor integral (cf. Kato [8, p. 44] or Taylor [17, pp. 287 ff.]) as follows:

$$(13) \quad f(A) = \frac{1}{2\pi i} \int_{\Gamma} f(\lambda)(\lambda - A)^{-1} d\lambda$$

or

$$(14) \quad f(A) = \frac{1}{2\pi i} \int_{\Gamma} f(\lambda)R_{\lambda} d\lambda$$

with

$$(15) \quad R_{\lambda} = (\lambda - A)^{-1}.$$

Analogously to Subsection 1.1, we define

$$(16) \quad I(f(A))_{[a,b]} := \frac{1}{2\pi i} \int_a^b f(\lambda)R_{\lambda} d\lambda.$$

Then, one gets the Gaussian quadrature formula

$$(17) \quad Q_{G_3}(f(A))_{[a,b]} = \frac{b-a}{2\pi i} \frac{1}{18} \left[5f\left(c - h\frac{\sqrt{15}}{5}\right)R_{c-h(\sqrt{15}/5)} + 8f(c)R_c + 5f\left(c + h\frac{\sqrt{15}}{5}\right)R_{c+h(\sqrt{15}/5)} \right].$$

Let $\|\cdot\|$ be a matrix norm. Then

(18)

$$\begin{aligned} \|E_{G_3}f(A)_{[a,b]}\| &\leq \frac{|b-a|^7}{2\pi} \frac{1}{2016000} \\ &\cdot \max_{s_a \leq s \leq s_b} \left\{ \left| \frac{d^6 f(\lambda(s))}{d\lambda^6} \right| \|R_{\lambda(s)}\| + 6 \left| \frac{d^5 f(\lambda(s))}{d\lambda^5} \right| \|R_{\lambda(s)}\|^2 \right. \\ &\quad + 30 \left| \frac{d^4 f(\lambda(s))}{d\lambda^4} \right| \|R_{\lambda(s)}\|^3 + 120 \left| \frac{d^3 f(\lambda(s))}{d\lambda^3} \right| \|R_{\lambda(s)}\|^4 \\ &\quad + 360 \left| \frac{d^2 f(\lambda(s))}{d\lambda^2} \right| \|R_{\lambda(s)}\|^5 + 720 \left| \frac{df(\lambda(s))}{d\lambda} \right| \|R_{\lambda(s)}\|^6 \\ &\quad \left. + 720 |f(\lambda(s))| \|R_{\lambda(s)}\|^7 \right\}. \end{aligned}$$

2.2 Summed quadrature formula on interval. For N subintervals, one gets

(19)

$$\begin{aligned} Q_{G_3}(f(A))_{[a,b]} &= \frac{1}{2\pi i} \frac{h}{9} \sum_{j=1}^N \left[5f\left(c_j - h \frac{\sqrt{15}}{5}\right) R_{c_j - h(\sqrt{15}/5)} + 8f(c_j) R_{c_j} \right. \\ &\quad \left. + 5f\left(c_j + h \frac{\sqrt{15}}{5}\right) R_{c_j + h(\sqrt{15}/5)} \right] \end{aligned}$$

with

$$\begin{aligned} \|E_{G_3}f(A)_{[a,b]}\| &\leq \frac{|b-a|^7}{2\pi N^6} \frac{1}{2016000} \\ &\cdot \max_{s_a \leq s \leq s_b} \left\{ \left| \frac{d^6 f(\lambda(s))}{d\lambda^6} \right| \|R_{\lambda(s)}\| + 6 \left| \frac{d^5 f(\lambda(s))}{d\lambda^5} \right| \|R_{\lambda(s)}\|^2 \right. \\ &\quad + 30 \left| \frac{d^4 f(\lambda(s))}{d\lambda^4} \right| \|R_{\lambda(s)}\|^3 + 120 \left| \frac{d^3 f(\lambda(s))}{d\lambda^3} \right| \|R_{\lambda(s)}\|^4 \\ &\quad + 360 \left| \frac{d^2 f(\lambda(s))}{d\lambda^2} \right| \|R_{\lambda(s)}\|^5 + 720 \left| \frac{df(\lambda(s))}{d\lambda} \right| \|R_{\lambda(s)}\|^6 \\ &\quad \left. + 720 |f(\lambda(s))| \|R_{\lambda(s)}\|^7 \right\}. \end{aligned}$$

2.3 Summed quadrature formula on closed polygonal. If the closed polygonal consists of K intervals $[a_k, b_k]$, $k = 1, \dots, K$, one has

$$(21) \quad Q(f(A)) = \sum_{k=1}^K Q(f(A))_{[a_k, b_k]}$$

and

$$(22) \quad \|E(f(A))\| \leq \sum_{k=1}^K \|E(f(A))_{[a_k, b_k]}\|.$$

3. A mechanical problem. There are many applications of the matrix exponential in mechanics. For example, the problem

$$\dot{x}(t) = Ax(t), \quad x(0) = x_0$$

with an $m \times m$ matrix A has the solution $x(t) = \Phi(t)x_0$ with $\Phi(t) = e^{At}$ (cf. Müller and Schiehlen [11, p. 73] or Bremer [2, p. 149]). Further,

$$\dot{x} = Ax(t) + b(t), \quad x(0) = x_0$$

is solved by

$$x(t) = \Phi(t)x_0 + \int_0^t \Phi(t - \tau)b(\tau) d\tau,$$

(cf. [11, p. 75] or [2, p. 158]). Remarks on the calculation of the fundamental matrix are made in [11, pp. 350–352].

Moreover, special cases of excitations are discussed in 11. For example, the impulse, step and harmonic excitations are described there on pages 189, 191–195, and 195–202, respectively.

In Pestel and Leckie [14, p. 141], a problem of elasticity involving the differential equation $(dz/ds) = Az + a(s)$ is treated.

See also the use of the fundamental matrix in Waller and Krings [18, e.g., p. 59], and of the matrix functions $\cos At$ and $\sin At$ [18, p. 53].

3.1 Free mechanical vibrations. We have seen that there is a whole range of applications involving the matrix exponential. For the sake of brevity, we restrict ourselves to the first example.

(i) *The example model.* We investigate the initial value problem

$$(23) \quad M\ddot{y} + B\dot{y} + Ky = 0$$

$$(24) \quad y(0) = y_0, \quad \dot{y}(0) = \dot{y}_0,$$

(cf. Müller and Schiehlen [11, pp. 46 ff.]) where (1) is the equation of motion of a mechanical system with the mass matrix M , the damping matrix B and the stiffness matrix K of dimension $n \times n$ as well as the displacement vector y of dimension n and where (24) are the initial conditions.

Introducing the state vector of dimension m ,

$$(25) \quad x(t) = \begin{bmatrix} y(t) \\ \dot{y}(t) \end{bmatrix} = \begin{bmatrix} y(t) \\ z(t) \end{bmatrix} \quad \text{with } z(t) = \dot{y}(t),$$

and the $m \times m$ system matrix

$$(26) \quad A = \left[\begin{array}{c|c} 0 & E \\ \hline -M^{-1}K & -M^{-1}B \end{array} \right]$$

with the identity matrix E , one obtains the state equation

$$(27) \quad \dot{x}(t) = Ax(t), \quad x(0) = x_0,$$

where we have assumed that M^{-1} exists and where $m = 2n$. More specifically, we consider the multi-mass vibration chain according to Figure 3.

Here, one has

$$(28) \quad M = \begin{bmatrix} m_1 & & & & \\ & m_2 & & & \\ & & m_3 & & \\ & & & \ddots & \\ & & & & m_n \end{bmatrix},$$

$$(29) \quad B = \begin{bmatrix} b_1 + b_2 & -b_2 & & & & \\ -b_2 & b_2 + b_3 & -b_3 & & & \\ & -b_3 & b_3 + b_4 & -b_4 & & \\ & & \ddots & \ddots & \ddots & \\ & & & -b_{n-1} & b_{n-1} + b_n & -b_n \\ & & & & -b_n & b_n + b_{n+1} \end{bmatrix},$$

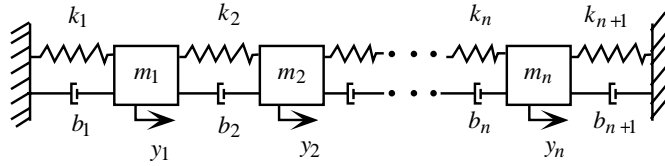


FIGURE 3. Multi-mass vibration chain.

$$(30) \quad K = \begin{bmatrix} k_1 + k_2 & -k_2 & & & \\ -k_2 & k_2 + k_3 & -k_3 & & \\ & -k_3 & k_3 + k_4 & -k_4 & \\ & & \ddots & \ddots & \ddots \\ & & & -k_{n-1} & k_{n-1} + k_n & -k_n \\ & & & -k_n & k_n + k_{n+1} & \end{bmatrix}.$$

(ii) *The test data.* To generate test data, we set

$$(31) \quad \begin{aligned} m_j &= m = 1, & j &= 1, \dots, n \\ k_j &= k = 1, & j &= 1, \dots, n \end{aligned}$$

and

$$b_j = \begin{cases} 1/2 & \text{if } j \text{ even} \\ 1/4 & \text{if } j \text{ odd.} \end{cases}$$

Then,

$$M = E,$$

$$(32) \quad B = \begin{bmatrix} 3/4 & -1/2 & & & \\ -1/2 & 3/4 & -1/4 & & \\ & -1/4 & 3/4 & -1/2 & \\ & & \ddots & \ddots & \ddots \\ & & & -1/4 & 3/4 & -1/2 \\ & & & & -1/2 & 3/4 \end{bmatrix},$$

(if n is even), and

$$(33) \quad K = \begin{bmatrix} 2 & -1 & & & \\ -1 & 2 & -1 & & \\ & -1 & 2 & -1 & \\ & & \ddots & \ddots & \ddots \\ & & & -1 & 2 & -1 \\ & & & & -1 & 2 \end{bmatrix}$$

Apparently, we have $B \neq \alpha M + \beta K$ and $B M^{-1} K \neq K M^{-1} B$ (cf. [11, p. 160, (6.69)]). We remark that the set of test data could be made more general by introducing the equation $b^2 = km$ as in Falk [4, p. 454].

As initial values, we choose

$$(34) \quad y_0 = [1 \ 1 \ \dots \ 1]^T$$

and

$$(35) \quad \dot{y}_0 = [0 \ 0 \ \dots \ 0]^T.$$

3.2 Numerical operational calculus.

(i) *Explanation of the numerical solution idea.* Since the function $f(z) = e^{zt}$ is analytic for fixed $t \geq 0$, there holds

$$(36) \quad e^{At} = \frac{1}{2\pi i} \int_{\Gamma} e^{\lambda t} R_{\lambda} d\lambda$$

where Γ is, for example, a closed polygonal and where the eigenvalues of A lie in the interior of Γ .

At first glance, this formula seems to be inadequate for the numerical evaluation because one has to calculate a contour integral in the complex plane, which takes a lot of operations.

But, a closer look at (36) tells us that one can take into account the special structure of A in the solution $x(t) = e^{At}x_0$. Indeed, one obtains

$$(37) \quad \begin{aligned} x(t) &= \frac{1}{2\pi i} \int_{\Gamma} e^{\lambda t} (\lambda - A)^{-1} x_0 d\lambda \\ &= \frac{1}{2\pi i} \int_{\Gamma} e^{\lambda t} R_{\lambda} x_0 d\lambda \\ &= \frac{1}{2\pi i} \int_{\Gamma} e^{\lambda t} u(\lambda) d\lambda \end{aligned}$$

where $u(\lambda)$ is the solution of

$$(38) \quad (\lambda - A)u(\lambda) = x_0.$$

In (38), the structure of A can be exploited. Setting

$$(39) \quad u(\lambda) =: u = \begin{bmatrix} v \\ w \end{bmatrix} \quad \text{and} \quad x_0 = \begin{bmatrix} y_0 \\ z_0 \end{bmatrix},$$

equation (38) is equivalent to

$$(40) \quad \left[\begin{array}{c|c} \lambda E & -E \\ \hline M^{-1}K & \lambda E + M^{-1}B \end{array} \right] \begin{bmatrix} v \\ w \end{bmatrix} = \begin{bmatrix} y_0 \\ z_0 \end{bmatrix}$$

or

$$(41) \quad \begin{aligned} Cv &= d_0 \\ w &= \lambda v - y_0 \end{aligned}$$

with

$$(42) \quad \begin{aligned} C &= C(\lambda) = \lambda^2 M + \lambda B + K = \lambda(\lambda M + B) + K \\ d_0 &= d_0(\lambda) = (\lambda M + B)y_0 + Mz_0. \end{aligned}$$

For example, if M , B and K have small bandwidth, so has $C = C(\lambda)$; especially, if M , B and K are tridiagonal, so is $C = C(\lambda)$. The solution $x(t) = [y(t)^T, z(t)^T]^T = [y(t)^T, \dot{y}(t)^T]^T$ is then given by

$$(43) \quad \begin{aligned} y(t) &= \frac{1}{2\pi i} \int_{\Gamma} e^{\lambda t} v(\lambda) d\lambda, \\ \dot{y}(t) &= \frac{1}{2\pi i} \int_{\Gamma} e^{\lambda t} w(\lambda) d\lambda. \end{aligned}$$

The idea described for the calculation of $(\lambda - A)^{-1}x_0$ (especially so as not to invert the matrix) also forms the basis of the numerical evaluation of the contour line, which we call numerical operational calculus. The equation (38), respectively (41), is solved here by the Gaussian elimination method. In the case of tridiagonal matrices, the number of multiplicative operations is essentially proportional to n , respectively m .

(ii) *The summed quadrature formula.* The summed Gaussian quadrature formula for expression (37) is obtained from (19) for $f(z) = e^{zt}$:

(44)

$$\begin{aligned} x_{G_3}(t) := \\ Q_{G_3}(f(A))_{[a,b]}x_0 &= \frac{1}{2\pi i} \frac{h}{9} \sum_{j=1}^N \left[5f\left(c_j - h\frac{\sqrt{15}}{5}\right) R_{c_j - h(\sqrt{15}/5)} x_0 \right. \\ &\quad \left. + 8f(c_j) R_{c_j} x_0 + 5f\left(c_j + h\frac{\sqrt{15}}{5}\right) \right. \\ &\quad \left. \cdot R_{c_j + h(\sqrt{15}/5)} x_0 \right]. \end{aligned}$$

where the quantities $R_{c_j - h(\sqrt{15}/5)} x_0$, $R_{c_j} x_0$, and $R_{c_j + h(\sqrt{15}/5)} x_0$ are evaluated as described above.

3.3. Upper bounds on norm of resolvent. In this subsection, let $\|\cdot\|$ be a norm for vectors in \mathbf{C}^n and $\|x\| := \max\{\|y\|, \|z\|\}$, $x = (y^T, z^T)^T \in \mathbf{C}^m = \mathbf{C}^{2n}$ a norm in \mathbf{C}^m .

For the estimates of the quadrature-formula error (i.e., the discretization error) in the next section, upper bounds of the resolvent, R_λ , in the norm $\|R_\lambda\| := \sup_{0 \neq x \in \mathbf{R}^m} \|R_\lambda x\|/\|x\|$ are needed, where λ ranges over the integration intervals.

In this subsection, we derive such bounds by taking into account the special structure and properties of A as well as the special properties of λ on the eigenvalue-adapted integration path.

Finally, it is assumed that the matrix M is invertible.

(i) *Using the special structure and special properties of matrix A .* Starting from (41), we get

$$\begin{aligned} \|d_0\| &= \|Cv\| = \|(\lambda^2 M + \lambda B + K)v\| \\ &\geq (|\lambda|^2 \|M^{-1}\|^{-1} - |\lambda| \|B\| - \|K\|) \|v\|, \end{aligned}$$

taking into account $d_0 = (\lambda M + B)y_0 + Mz_0$; this leads to

$$(45) \quad \|v\| \leq \frac{|\lambda| \|M\| + \|B\| + \|M\|}{|\lambda|^2 \|M^{-1}\|^{-1} - |\lambda| \|B\| - \|K\|} \|x_0\|$$

provided that the denominator is greater than zero.

Further, from the equation $Cw = -Ky_0 + \lambda Mz_0$ one infers similarly

$$(46) \quad \|w\| \leq \frac{|\lambda| \|M\| + \|K\|}{|\lambda|^2 \|M^{-1}\|^{-1} - |\lambda| \|B\| - \|K\|} \|x_0\|$$

Consequently, one has

$$(47) \quad \begin{aligned} \|v(\lambda)\| &\leq \hat{q} \|x_0\| \\ \|w(\lambda)\| &\leq \tilde{q} \|x_0\| \end{aligned}$$

as well as

$$(48) \quad \|u\| \leq q \|x_0\|, \quad \text{resp. } \|R_\lambda x_0\| \leq q \|x_0\|, \quad \text{resp. } \|R_\lambda\| \leq q$$

with

$$(49) \quad q = \max\{\hat{q}, \tilde{q}\}, \quad \begin{cases} \hat{q} := \frac{|\lambda| \|M\| + \|B\| + \|M\|}{|\lambda|^2 \|M^{-1}\|^{-1} - |\lambda| \|B\| - \|K\|} \\ \tilde{q} := \frac{|\lambda| \|M\| + \|K\|}{|\lambda|^2 \|M^{-1}\|^{-1} - |\lambda| \|B\| - \|K\|}. \end{cases}$$

For the test data, in the maximum norm we obtain $\|M\|_\infty = 1$, $\|M^{-1}\|_\infty^{-1} = 1$, $\|B\| = \|B\|_\infty = 1.5$ and $\|K\| = \|K\|_\infty = 4$ as well as $\|x\| = \max\{\|y\|_\infty, \|z\|_\infty\} = \|x\|_\infty$.

(ii) *Using the eigenvalue-adapted path.* Now, the quantity $q = q(d) = q(d, \lambda)$ must be estimated further from the above. Using the eigenvalue-adapted path 1 in Figure 4, the estimates on the four intervals can be derived and represented in a unified way. We obtain $q \leq q_k$ where

$$(50) \quad q_k = \max\{\hat{q}_k, \tilde{q}_k\}, \quad \begin{cases} \hat{q}_k := \frac{\delta_k(d) \|M\| + \|B\| + \|M\|}{\delta_k^2(d) \|M^{-1}\|^{-1} - \delta_k(d) \|B\| - \|K\|} \\ \tilde{q}_k := \frac{\delta_k(d) \|M\| + \|K\|}{\delta_k^2(d) \|M^{-1}\|^{-1} - \delta_k(d) \|B\| - \|K\|}. \end{cases}$$

$$\delta_k(d) = \begin{cases} d, & k = 1 \\ \frac{\tilde{\rho}_y}{2} + d, & k = 2 \\ \tilde{\rho}_x + d, & k = 3 \\ \frac{\tilde{\rho}_y}{2} + d, & k = 4 \end{cases}$$

provided that the denominators are greater than zero.

We derive (50) only for $k = 1$. In this case, $\lambda = d + i\lambda_i$, $|\lambda| = \sqrt{d^2 + \lambda_i^2}$, $-(\tilde{\rho}_y/2) + d \leq \lambda_i \leq (\tilde{\rho}_y/2) + d$. Therefore, from (49)

$$\begin{aligned} \hat{q}_1 &= \frac{\sqrt{d^2 + \lambda_i^2} \|M\| + \|B\| + \|M\|}{(d^2 + \lambda_i^2) \|M^{-1}\|^{-1} - \sqrt{d^2 + \lambda_i^2} \|B\| - \|K\|} \\ &= \frac{\|M\| + (\|B\| + \|M\|)/\sqrt{d^2 + \lambda_i^2}}{\sqrt{d^2 + \lambda_i^2} \|M^{-1}\|^{-1} - \|B\| - (\|K\|/\sqrt{d^2 + \lambda_i^2})} \\ &\leq \frac{d\|M\| + \|B\| + \|M\|}{d^2 \|M^{-1}\|^{-1} - d\|B\| - \|K\|}; \end{aligned}$$

similarly,

$$\tilde{q}_1 \leq \frac{d\|M\| + \|K\|}{d^2 \|M^{-1}\|^{-1} - d\|B\| - \|K\|}.$$

So (50) is proven. \square

Remark. The denominator in (45) is positive for $\lambda \in [a_k, b_k]$ if the denominator in (50) is positive and $\delta_k(d) > (\|B\| \|M^{-1}\|/2)$.

3.4. Estimates of the discretization error. In this subsection we first state the error estimates on the four intervals making up the eigenvalue-adapted path. Then we show how these estimates can be used to calculate the quantities $d = d_{\min}$ and $N(k)$, $k = 1, \dots, 4$ (cf. Figure 4).

We obtain on *Interval 1*:

(51)

$$\|E_{G_3}(e^{At})_{[a_1, b_1]} x_0\| \leq \frac{1}{N(1)^6} \frac{1}{2\pi} \frac{1}{2016000} (\tilde{\rho}_y + 2d)^7 e^{dt} \chi(q_1(d), t) \|x_0\|$$

with

$$(52) \quad \chi(q, t) := qt^6 + 6q^2t^5 + 30q^3t^4 + 120q^4t^3 + 360q^5t^2 + 720q^6t + 720q^7,$$

on *Interval 3*:

$$(53) \quad \|E_{G_3}(e^{At})_{[a_3, b_3]} x_0\| \leq \frac{1}{N(3)^6} \frac{1}{2\pi} \frac{1}{2016000} (\tilde{\rho}_y + 2d)^7 e^{-(\tilde{\rho}_x + d)t} \cdot \chi(q_3(d), t) \|x_0\|,$$

and on *Intervals* k , $k = 2, 4$ (starting with the estimates of Section 2.1, not 2.2):

$$(54) \quad \|E_{G_3}(e^{At})_{[a_k, b_k]}x_0\| \leq \frac{e^{(\tilde{\rho}_x+2d)t/N(k)}}{N(k)^6} \frac{1}{2\pi} \frac{1}{2016000} (\tilde{\rho}_x+2d)^6 \cdot \frac{(e^{dt} - e^{-(\tilde{\rho}_x+d)t})}{t} \chi(q_k(d), t) \|x_0\|.$$

We remark that $\lim_{t \rightarrow 0} (e^{dt} - e^{-(\tilde{\rho}_x+d)t})/t = \tilde{\rho}_x + 2d$.

With these error estimates, $d = d_{\min}$ as well as the numbers $N(k)$, $k = 1, \dots, 4$, of subdivisions can be determined.

As a consequence, the described method is of order $O(N(k)^{-6})$ on Interval k , $k = 1, \dots, 4$.

Determination of d_{\min} and $N(1)$. Let $t > 0$ be fixed (for example, $t = 1$) and let

$$(55) \quad h_1(d) := \frac{1}{2\pi} \frac{1}{2016000} (\tilde{\rho}_y + 2d)^7 e^{dt} \chi(q_1(d), t) \|x_0\|.$$

Then, d_{\min} is determined as

$$(56) \quad h_1(d_{\min}) = \min_{\tilde{d}_{\min} \leq d \leq \tilde{d}_{\max}} h_1(d),$$

where $\tilde{d}_{\min} > 0$, respectively $\tilde{d}_{\max} > 0$ is sufficiently small, respectively large. For given $\varepsilon > 0$ (here, $\varepsilon = 0.5 \cdot 10^{-4}$), $N(1)$ is determined from

$$(57) \quad \frac{h_1(d_{\min})}{N(1)^6} = \frac{\varepsilon}{4} =: \varepsilon_4$$

so that

$$(58) \quad N(1) = \sqrt[6]{\frac{h_1(d_{\min})}{\varepsilon_4}}.$$

We remark that the relative error is minimized on Interval 1 since it is much larger there than on the other intervals. Further, we mention

that, near $d = d_{\min}$, the function $h_1(d)$ is flat, which means that the discretization error is insensitive to small deviations from $d = d_{\min}$.

Determination of $N(3)$. Let

$$(59) \quad h_3(d) := \frac{1}{2\pi} \frac{1}{2016000} (\tilde{\rho}_y + 2d)^7 e^{-(\tilde{\rho}_x + d)t} \chi(q_3(d), t) \|x_0\|$$

for fixed $t > 0$. Then, $N(3)$ is computed as

$$(60) \quad N(3) = \sqrt[6]{\frac{h_3(d_{\min})}{\varepsilon_4}}.$$

Determination of $N(k)$, $k = 2, 4$. For fixed $t > 0$ and $d = d_{\min}$, let $h(N(k))$, $k = 2, 4$, be the righthand side in (54). Then, $N(k)$ is computed numerically in such a way that

$$(61) \quad h_k(N(k)) = \varepsilon_4, \quad k = 2, 4$$

which is done in the example of the next section by the Newton method.

After having been determined, the numbers $N(k)$, $k = 1, \dots, 4$ are rounded up, as a rule.

3.5 Computational results. In this subsection we take the test data from Subsection 3.1, i.e., $M = E$ and (32)–(35). Then, independently of the dimension number n resp $m = 2n$, the eigenvalues of A lie in the inner of the dashed rectangle in Figure 4 (cf. Falk [4, Figure 8]). *Path 1* consists of four axis-parallel intervals as indicated in Figure 4. The horizontal and vertical distance of these intervals to the sides of the inner rectangle is denoted as d .

Only in this section, we use the condition that the matrices M , B and K are sparse.

For some matrix orders m ranging between $m = 10$ and $m = 1000$, the associated computation times are determined.

First, two algorithms which are assessed to be among the better ones for the computation of the matrix exponential in [6, p. 560] were compared. These are algorithm 11.3.1 (Ward's implementation of scaling

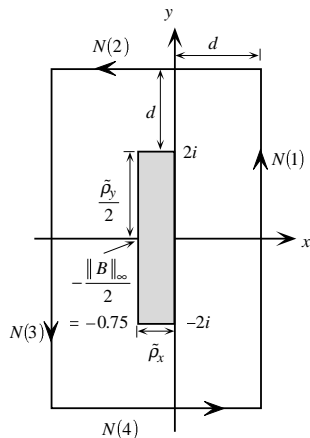


FIGURE 4. Path 1 and numbers $N(k)$ of subdivisions on intervals $[a_k, b_k]$, $k = 1, \dots, 4$.

and squaring with Padé approximants) and algorithm 11.1.1 (implementation of Parlett’s Schur decomposition). In MATLAB, the associated functions are *expm1* and *funm(·, 'exp')*. Ward’s implementation was faster.

So, in Table 1 only the results for the described method and Ward’s method (called SCALING AND SQUARING in [10]) are compiled.

Since the number of multiplicative operations in the numerical operational calculus is essentially proportional to n and those in Ward’s method are roughly proportional to n^3 (cf. [10]), one can expect the new method to be much faster for sufficiently large n . This is confirmed by the results in Table 1.

For $n = 5$, that is $m = 10$, both methods give

$$x(t = 1) = [+0.6516, +0.9230, +0.9849, +0.9470, +0.6583, \\ -0.5384, -0.2125, -0.0617, -0.1579, -0.5141].$$

In Ward’s method, the special structure of the matrix A could be taken into account, and it could thus be made somewhat faster. But nevertheless its band width would be much greater than that of NOC. However, Ward’s method would compare more favorably with NOC if in MATLAB $e^A b$ was programmed and not only e^A .

TABLE 1. Numerical Operational Calculus (left),
respectively Ward's method (right)

Norm	: $\ x\ = \ x\ _\infty, x = [y^T, z^T]^T$
Path	: Path 1 in Figure 4 with $\tilde{\rho}_y/2 = 2$, $\tilde{\rho}_x = 0.75, d = d_{\min} = 5.7562$, $t = 1$, and $\varepsilon = 0.5 \cdot 10^{-4}$
$N(k), k = 1, \dots, 4$: $N(1) = 50, N(2) = 19, N(3) = 6, N(4) = 19$
Hardware	: CPU-Time 66 MHz, High-Speed Memory 20 MBytes
Software	: 368-Matlab, 4.2c
Plot of Results	: Curve NOC, respectively, Curve W in Figure 5

n	$m = 2n$	$t[s] = t_{\text{NOC}}$	$t[s] = t_W$
5	10	4.89	0.05
10	20	8.46	0.17
15	30	12.19	0.39
20	40	15.33	0.71
25	50	18.67	1.21
30	60	22.02	1.82
35	70	25.60	2.86
40	80	29.00	4.94
45	90	32.63	5.82
50	100	36.14	7.80
75	150	54.76	26.37
100	200	74.37	97.39
150	300	114.30	423.42
200	400	159.61	1 006.9
250	500	190.21	2 134.7
300	600	238.59	4 103.6
350	700	285.45	6 784.0
400	800	340.64	12 374.0
450	900	405.02	*
500	1000	469.01	

* Run was manually interrupted after more than 21 600 s (=6 h) had elapsed.

4. Mathematical problems. In this section, we demonstrate the Numerical Operational Calculus for some mathematical problems. We do not claim, for these examples, its superiority to other methods, but

we just want to show that the discussed problems can be solved in a straightforward manner, by the method described.

In Subsection 4.1, we compute an example of Stickel on a matrix e^A . In Subsection 4.2, the spectral decomposition of the same matrix A as in 4.1 is computed. Finally, in Subsection 4.3, we calculate the square root of a matrix A in [16].

For the sake of brevity and simplicity, we do not estimate the error, but make numerical experiments instead of determining the numbers $N(k)$ on intervals $[a_k, b_k]$, $k = 1, \dots, 4$.

4.1 The matrix exponential example of Stickel. In [15], Stickel calculates the matrix exponential of

$$A = \begin{bmatrix} 10 & -19 & 17 & -12 & 4 & 1 \\ 9 & -18 & 17 & -12 & 4 & 1 \\ 8 & -16 & 15 & -11 & 4 & 1 \\ 6 & -12 & 12 & -10 & 4 & 1 \\ 4 & -8 & 8 & -6 & 1 & 2 \\ 2 & -4 & 4 & -3 & 1 & 0 \end{bmatrix}$$

which was taken from Gregory and Karney [7, p. 91]. With the path and data in Figure 6, we obtain

$$e^A = \begin{bmatrix} 16.9741 & -24.0070 & 12.2979 & -6.0007 & 0.9197 & 1.4715 \\ 14.2558 & -21.2887 & 12.2979 & -6.0007 & 0.9197 & 1.4715 \\ 12.0778 & -18.8096 & 11.1552 & -5.1592 & 0.9197 & 1.4715 \\ 9.0584 & -14.1072 & 8.0905 & -3.7774 & 0.9197 & 1.4715 \\ 6.0389 & -9.4048 & 5.3937 & -2.7635 & 0.7358 & 1.4715 \\ 3.0195 & -4.7024 & 2.6968 & -1.3818 & 0.1839 & 1.1036 \end{bmatrix}.$$

The result of Stickel is

$$e^A = \begin{bmatrix} 16.974 & -24.007 & 12.298 & -6.001 & 0.920 & 1.472 \\ 14.256 & -21.289 & 12.298 & -6.001 & 0.920 & 1.472 \\ \mathbf{12.256} & -18.810 & 11.155 & -5.159 & 0.920 & 1.472 \\ \mathbf{9.078} & -14.107 & 8.091 & -3.777 & 0.920 & 1.472 \\ 6.039 & -9.405 & 5.394 & -2.764 & 0.736 & 1.472 \\ 3.019 & -4.702 & 2.697 & -1.382 & 0.184 & 1.104 \end{bmatrix}.$$

The entries (3,1) and (4,1) in bold face are misprinted, as has been confirmed by Stickel in a private letter. We remark that, since the

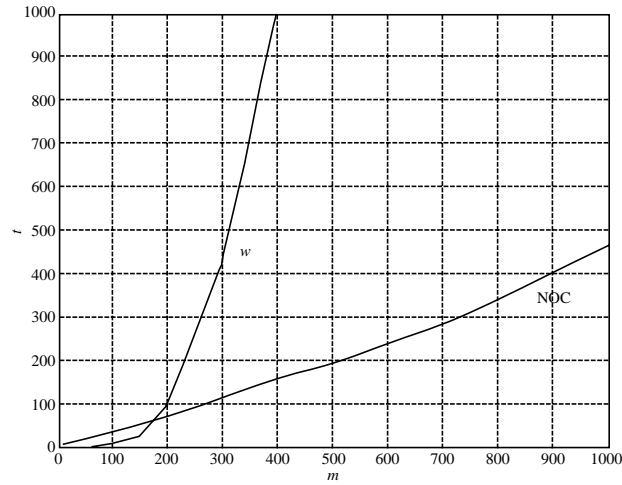


FIGURE 5. Curves NOC and W.

eigenvalue λ_4 is threefold, it is appropriate to choose $N(1) = N(2) = N(3) = N(4)$.

4.2 Spectral decomposition of a matrix. According to Kato [8, p. 41], the spectral decomposition of the matrix A in Subsection 4.1 is

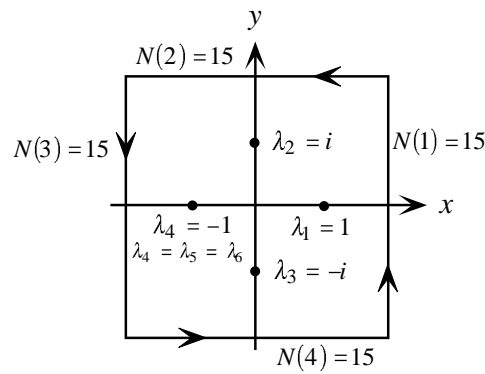


FIGURE 6. Path 2 and numbers $N(k)$ of subdivisions on intervals $[a_k, b_k]$, $k = 1, \dots, 4$.

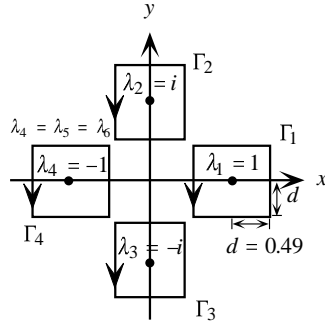


FIGURE 7. Path 3: Number of subdivisions on each interval is $N = 15$.

given by

$$A = \sum_{k=1}^4 \lambda_k P_{\lambda_k} + D$$

with

$$D = \sum_{k=1}^4 D_{\lambda_k}; \quad D_{\lambda_k} = \frac{1}{2\pi i} \int_{\Gamma_k} (\lambda - \lambda_k) R_{\lambda} d\lambda, \quad k = 1, \dots, 4$$

where D_{λ_k} are nilpotent and where

$$P_{\lambda_k} = \frac{1}{2\pi i} \int_{\Gamma_k} R_{\lambda} d\lambda, \quad k = 1, \dots, 4;$$

are projections with Γ_k taken from Figure 7.

The result (correct up to four decimal digits) is

$$P_{\lambda_1} = \begin{bmatrix} 6 & -6 & 0 & 0 & 0 & 0 \\ 5 & -5 & 0 & 0 & 0 & 0 \\ 4 & -4 & 0 & 0 & 0 & 0 \\ 3 & -3 & 0 & 0 & 0 & 0 \\ 2 & -2 & 0 & 0 & 0 & 0 \\ 1 & -1 & 0 & 0 & 0 & 0 \end{bmatrix},$$

$$P_{\lambda_2} = \begin{bmatrix} -2.5 - 2.0i & 3.0 + 6.5i & 1.5 - 7.0i & -2.0 + 2.5i & 0.0 & 0.0 \\ -2.5 - 2.0i & 3.0 + 6.5i & 1.5 - 7.0i & -2.0 + 2.5i & 0.0 & 0.0 \\ -2.0 - 2.0i & 2.0 + 6.0i & 2.0 - 6.0i & -2.0 + 2.0i & 0.0 & 0.0 \\ -1.5 - 1.5i & 1.5 + 4.5i & 1.5 - 4.5i & -1.5 + 1.5i & 0.0 & 0.0 \\ -1.0 - 1.0i & 1.0 + 3.0i & 1.0 - 3.0i & -1.0 + 1.0i & 0.0 & 0.0 \\ -0.5 - 0.5i & 0.5 + 1.5i & 0.5 - 1.5i & -0.5 + 0.5i & 0.0 & 0.0cr \end{bmatrix},$$

$$\begin{aligned}
P_{\lambda_3} &= \begin{bmatrix} -2.5 + 2.0i & 3.0 - 6.5i & 1.5 + 7.0i & -2.0 - 2.5i & 0.0 & 0.0 \\ -2.5 + 2.0i & 3.0 - 6.5i & 1.5 + 7.0i & -2.0 - 2.5i & 0.0 & 0.0 \\ -2.0 + 2.0i & 2.0 - 6.0i & 2.0 + 6.0i & -2.0 - 2.0i & 0.0 & 0.0 \\ -1.5 + 1.5i & 1.5 - 4.5i & 1.5 + 4.5i & -1.5 - 1.5i & 0.0 & 0.0 \\ -1.0 + 1.0i & 1.0 - 3.0i & 1.0 + 3.0i & -1.0 - 1.0i & 0.0 & 0.0 \\ -0.5 + 0.5i & 0.5 - 1.5i & 0.5 + 1.5i & -0.5 - 0.5i & 0.0 & 0.0 \end{bmatrix} = \overline{P}_{\lambda_2}, \\
P_{\lambda_4} &= \begin{bmatrix} 0.0 & 0.0 & -3.0 & 4.0 & 0.0 & 0.0 \\ 0.0 & 0.0 & -3.0 & 4.0 & 0.0 & 0.0 \\ 0.0 & 0.0 & -3.0 & 4.0 & 0.0 & 0.0 \\ 0.0 & 0.0 & -3.0 & 4.0 & 0.0 & 0.0 \\ 0.0 & 0.0 & -2.0 & 2.0 & 1.0 & 0.0 \\ 0.0 & 0.0 & -1.0 & 1.0 & 0.0 & 1.0 \end{bmatrix}, \\
D &= \begin{bmatrix} 0.0 & 0.0 & 0.0 & -3.0 & 4.0 & 1.0 \\ 0.0 & 0.0 & 0.0 & -3.0 & 4.0 & 1.0 \\ 0.0 & 0.0 & 0.0 & -3.0 & 4.0 & 1.0 \\ 0.0 & 0.0 & 0.0 & -3.0 & 4.0 & 1.0 \\ 0.0 & 0.0 & 0.0 & -2.0 & 2.0 & 2.0 \\ 0.0 & 0.0 & 0.0 & -1.0 & 1.0 & 1.0 \end{bmatrix}.
\end{aligned}$$

It was checked that $A = \sum_{k=1}^4 \lambda_k P_{\lambda_k} + D$ is exact up to four digits.

We remark that the spectral decomposition of a matrix is also discussed in Niemeyer and Wermuth [12, pp. 235–237] for simple eigenvalues.

4.3 Square root of a positive definite matrix. In [16, p. 197], the square root of the matrix

$$A = \begin{bmatrix} 20 & -4 & -4 & -1 \\ -4 & 20 & -1 & -4 \\ -4 & -1 & 20 & -4 \\ -1 & -4 & -4 & 20 \end{bmatrix}$$

is calculated by the method of successive approximations. Here, we calculate it based on the representation $A^{1/2} = (1/2\pi i) \int_{\Gamma} \lambda^{1/2} R_{\lambda} d\lambda$. The eigenvalues of A are $\lambda_1 = 11$, $\lambda_2 = \lambda_3 = 21$, $\lambda_4 = 27$. Taking the path in Figure 8,

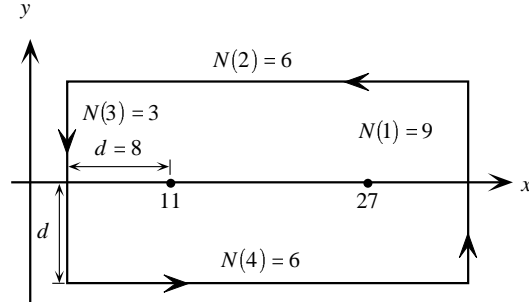


FIGURE 8. Path 4 and numbers $N(k)$ of subdivisions on intervals $[a_k, b_k]$, $k = 1, \dots, 4$.

we obtain

$$\sqrt{A} = \begin{bmatrix} 4.41948 & -0.46988 & -0.46988 & -0.16309 \\ -0.46988 & 4.41948 & -0.16309 & -0.46988 \\ -0.46988 & -0.16309 & 4.41948 & -0.46988 \\ -0.16309 & -0.46988 & -0.46988 & 4.41948 \end{bmatrix},$$

which is the same result as in [16].

5. Concluding remarks. Numerical Operational Calculus compares favorably to the other methods in case of positive definite matrices M , B and K where the eigenvalues of (M, B, K) can be enclosed, for example, by the results of Falk and where the bandwidth of the three matrices is small and the dimension n is large.

In the general case where the matrix A has no special structure the eigenvalues λ of A can be bounded by $|\lambda| \leq \|A\|$, where in the test example $\|A\|_\infty = 5.5$. Bounds on the resolvent are then given by $\|R_\lambda\| \leq (|\lambda| - \|A\|)^{-1}$, $|\lambda| > \|A\|$.

Most important, however, is that for Numerical Operational Calculus a backward error analysis can be given. This is due to the fact that we have essentially reduced the problem to the solution of linear equations.

For large values of time, say, $T = 25$, the interval $[0, T]$ is subdivided into small intervals of length Δt , say, $\Delta t = 0.2$, and the described method is used to transform $x(t_0) \rightarrow x(t_0 + \Delta t) = x(t_1)$, $x(t_1) \rightarrow x(t_1 + \Delta t) = x(t_2)$, and so on.

Also, the method can be used for excited vibrations.

REFERENCES

1. S. Baroni and G. Giannozzi, *Towards very large-scale electronic-structure calculations*, Europhys. Lett. **17** (1992), 547–552.
2. H. Bremer, *Dynamik und Regelung mechanischer Systeme*, B.G. Teubner, Stuttgart, 1988.
3. S. Falk, *Klassifikation gedämpfter Schwingungssysteme und Eingrenzung ihrer Elemente*, Ing.-Arch. **29**, (1960), 436–444.
4. ———, *Expansion von Polynomen und Polynommatrizen*, ZAMM **64** (1984), 445–456.
5. S. Goedecker, *Low complexity algorithms for electronic structure calculations*, J. Comp. Physics **118** (1995), 261–268.
6. G.H. Golub and C.F. van Loan, *Matrix computations*, The Johns Hopkins University Press, Baltimore, 1983.
7. R.T. Gregory and D.L. Karney, *A collection of matrices for testing computational algorithms*, Wiley-Interscience, New York, 1969.
8. T. Kato, *Perturbation theory for linear operators*, Springer, New York, 1986.
9. K. Knopp, *Funktionentheorie I (Grundlagen der allgemeinen Theorie der analytischen Funktionen)*, Walter de Gruyter, Berlin, 1965.
10. C.B. Mohler and C.F. van Loan, *Nineteen dubious ways to compute the exponential of a matrix*, SIAM Review **20** (1978), 801–836.
11. P.C. Müller and W.O. Schiehlen, *Lineare Schwingungen*, Akademische Verlagsgesellschaft, Wiesbaden, 1976.
12. H. Niemeyer and E. Wermuth, *Lineare Algebra – Analytische und numerische Behandlung*, Vieweg, Braunschweig Wiesbaden, 1987.
13. D.M.C. Nocholson, G.M. Stocks, Y. Wang, W.A. Shelton, Z. Szotek and W.M. Temmerman, *Stationary nature of density-functional free energy: Application of accelerated multiple-scattering calculations*, Phys. Rev. B **50** (1994), 14686–14689.
14. E.C. Pestel and F.A. Leckie, *Matrix methods in elastomechanics*, McGraw-Hill, New York, 1963.
15. E.U. Stickel, *A splitting method for the calculation of the matrix exponential*, Analysis **14** (1994), 103–112.
16. F. Stummel and K. Hainer, *Praktische Mathematik*, B.G. Teubner, Stuttgart, 1982.
17. A.E. Taylor, *Introduction to functional analysis*, John Wiley & Sons Inc., New York, 1958.
18. H. Waller and W. Krings, *Matrizendynamik in der Maschinen- und Bauwerksdynamik*, Bibliographisches Institut, Mannheim, Wien, Zürich, 1975.
19. J.H. Wilkinson, *The algebraic eigenvalue problem*, Clarendon Press, Oxford, 1965.
20. ———, *Rundungsfehler*, Springer, Berlin, 1969.
21. R. Zurmühl and S. Falk, *Matrizen und ihre Anwendungen, Teil 1 (Grundlagen)*, Springer, Berlin et al., 1984.

22. ———, *Matrizen und ihre Anwendungen, Teil 2 (Numerische Methoden)*, Springer, Berlin et al., 1986.

LUDWIG KOHAUPT, PRAGER STR. 9, D-10779 BERLIN, GERMANY
E-mail address: kohaupt@tfh-berlin.de